ChemComm

COMMUNICATION

View Article Online
View Journal | View Issue

Cite this: *Chem. Commun.*, 2019, 55, 9653

Received 7th May 2019,
Accepted 15th July 2019

DOI: 10.1039/c9cc03502h

rsc.li/chemcomm

A supersensitive biosensor based on MoS_2 nanosheet arrays for the real-time detection of H_2O_2 secreted from living cells†

Huitong Du, Xinyue Zhang, Zhe Liu and Fengli Qu *

The fast and accurate real-time monitoring of hydrogen peroxide (H_2O_2) secreted from living cells plays a critical role in clinical diagnosis and management. Herein, we report low-cost and self-supported MoS_2 nanosheet arrays for non-enzymatic eletrochemical H_2O_2 detection. Under the optimal test conditions, such MoS_2 electrodes exhibit extremely promising electrocatalytic performance with a low detection limit of 1.0 μM (S/N = 3) and an excellent sensitivity of 5.3 mA mM^{-1} cm^{-2}. Furthermore, the detection of the trace amount of H_2O_2 secreted from live A549 cancer cells was successfully performed with this biosensor.

Highly sensitive and effective determination of hydrogen peroxide (H_2O_2) concentration is of utmost importance in the fields of textile industries, bioanalysis, pharmaceutical security and environmental protection.[1,2] In particular, H_2O_2 is a critical small molecule involved in immune responses, cell growth and signal transduction in different biological tissues.[3–7]

The intracellular H_2O_2 concentration level is a key physiological parameter for early primary cancer screening and diagnosis, which opens a new horizon for reducing the mortality rate of cancer patients.[8] As a consequence, developing accurate and convenient analytical technologies for real-time H_2O_2 sensing is necessary and urgent *in vitro* and *in vivo*. Compared to conventional techniques for H_2O_2 detection including phosphorescence, fluorescence/luminescence,[9–14] chromatography,[15–17] and spectrophotometry,[18] numerous efforts have been devoted to designing and developing electrochemical sensing methods due to their advantages of simple operation, desirable selectivity and quick responsiveness. At present, enzyme-based electrochemical biosensors have attracted ever-increasing attention in terms of their high sensitivity and superior specificity. Nevertheless, most of the reported enzymatic sensors still suffer from intrinsic problems including complicated preparation procedures, low durability, and high cost, which have severely influenced their efficiency and limited their practical application.[19] In sharp contrast, enzyme-free electrochemical biosensors based on nanostructured materials exhibit long-term stability, a wide application range and quick responsiveness.[20,21] Although noble metal-based biosensors show excellent electrochemical detection performance, the limited storage and high cost hinder their widespread use.[22–25] Thus, it is highly attractive to build earth-abundant element-based biosensors to realize supersensitive detection.

In previous work, MoS_2 was reported as a high-performance catalyst for the hydrogen evolution reaction and the oxygen reduction reaction and presented promising potential for the construction of electrocatalytic biosensors due to its excellent electrocatalytic properties.[26,27]

Recently, MoS_2 nanoparticles and interlayer-expanded MoS_2 were designed as electrochemical biosensors for H_2O_2 detection with a low detection limit.[28,29] Although impressive H_2O_2 detection performance has been achieved, a prime challenge still lies in the sensitivity. The construction of self-supported nanoarrays has been proposed as an effective strategy to improve the electrochemical performance of nanomaterials by virtue of increasing the catalytic sites and enhancing the electronic conductivity and contact area.[30,31] Thus, we anticipate that the electrochemical sensing ability of MoS_2 can be further enhanced by constructing self-supported nanoarrays.

In this communication, we report the synthesis of MoS_2 nanosheet arrays grown on carbon cloth (MoS_2/CC) for supersensitive detecting of H_2O_2. Furthermore, the trace amount of H_2O_2 produced from live cells was successfully detected with this MoS_2/CC biosensor. Satisfactorily, the proposed MoS_2/CC electrochemical biosensor exhibits super sensing performance with a low detection limit of 1.0 μM (S/N = 3) and an excellent sensitivity of 5.3 mA mM^{-1} cm^{-2}. This work offers considerably significant guidance for designing biosensors in the field of electrochemical sensing.

Fig. 1a shows the X-ray diffraction (XRD) patterns of the resulting MoS_2/CC; several diffraction peaks of MoS_2/CC can be

College of Chemistry and Chemical Engineering, Qufu Normal University, Qufu 273165, Shandong, China. E-mail: fengliquhn@hotmail.com

† Electronic supplementary information (ESI) available: Experimental section and supplementary figures. See DOI: 10.1039/c9cc03502h

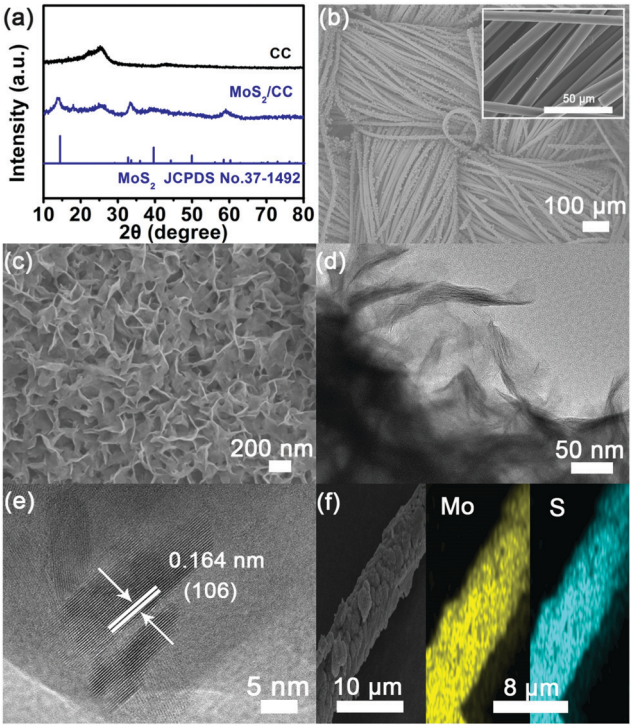

Fig. 1 (a) XRD patterns of CC and MoS_2/CC. (b and c) SEM images of CC (inset) and MoS_2/CC with different magnifications. TEM (d) and high-resolution TEM (e) images of MoS_2 nanosheets. (f) EDS elemental mapping images of Mo and S for MoS_2/CC.

assigned to the MoS_2 phase (JCPDS No. 37-1492). Additionally, the diffraction peak at 26.2° can be indexed to the bare CC substrate. No other diffraction peaks can be observed, indicating the high purity of the MoS_2/CC sample.

The scanning electron microscopy (SEM) image (Fig. 1b) indicates the full coverage of bare CC (inset) with MoS_2 nanosheets. The magnified SEM image (Fig. 1c) further reveals that MoS_2 has a typical sheet-like structure. The high-resolution TEM (HRTEM, Fig. 1e) image taken from the single nanosheet (Fig. 1d) shows a well-resolved lattice fringe with an interlayer spacing of 0.164 nm, corresponding to the (106) plane of the hexagonal MoS_2 crystals. The selected area electron diffraction (SAED) pattern (Fig. S1, ESI†) shows three diffraction rings indexed to the (004), (101) and (106) planes of the MoS_2 phase.

Additionally, the energy-dispersive X-ray (EDS) spectrum of MoS_2/CC indicates the co-existence of Mo and S elements with an atomic ratio of 0.35 : 0.65 (Fig. S2, ESI†). And the EDS elemental mapping analysis further confirms the uniform distribution of Mo and S elements within the whole nanoarrays (Fig. 1f). Furthermore, the X-ray photoelectron spectroscopy (XPS) survey spectrum of MoS_2/CC also confirms the presence of Mo and S elements (Fig. S3a, ESI†). In Fig. S3b (ESI†), the binding energies (BEs) at 232.2 and 229.1 eV correspond to Mo $3d_{3/2}$ and Mo $3d_{5/2}$ in the Mo 3d region, indicating the existence of Mo^{2+}.[32] The S 2s peaks located at 226.7 eV can also be seen in the Mo region. In Fig. S3c (ESI†), the S 2p spectrum shows two obvious peaks with BEs of 232.5 and 235.3 eV, attributed to S $2p_{3/2}$ and S $2p_{1/2}$ respectively, indicating the presence of S^{2-}.[33] The above observations collectively indicate the successful synthesis of MoS_2 nanosheet arrays.

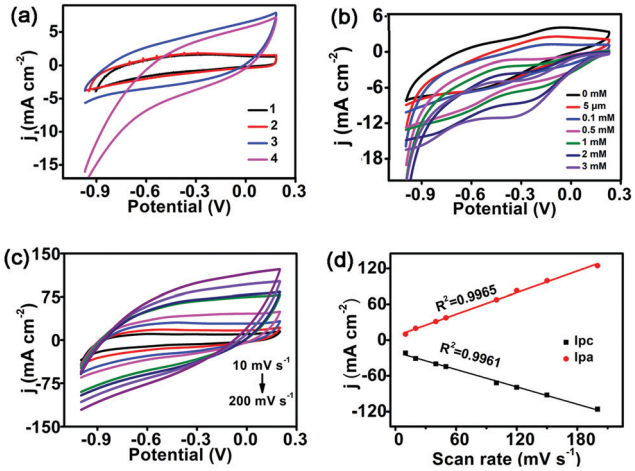

Fig. 2 (a) CVs of bare CC (curves 1 and 2) and MoS_2/CC (curves 3 and 4) in the absence and presence of 1 mM H_2O_2 in 0.1 M PBS (pH = 7.4) (scan rate: 50 mV s^{-1}). (b) CVs of MoS_2/CC in 0.1 M PBS with varying H_2O_2 concentrations. (c) CVs of MoS_2/CC in 0.1 M PBS containing 1 mM H_2O_2 at scan rates from 5 mV s^{-1} to 200 mV s^{-1}. (d) The corresponding plots of the current density *vs.* scan rates.

Cyclic voltammetry (CV) is preferably applied to reveal the catalytic activity of the designed biosensor for H_2O_2 reduction. In Fig. 2a, bare CC (curves 1 and 2) displays a nearly similar current density in the absence and presence of 1 mM H_2O_2 in 0.1 M PBS, indicating that the bare CC electrode is electrochemically inert for the detection of H_2O_2. In contrast, the reduction current density of the MoS_2/CC electrode (curves 3 and 4) is notably increased by ~200% after adding 1 mM H_2O_2, suggesting that the obtained MoS_2/CC electrode is feasible for H_2O_2 detection. As plotted in Fig. 2b, the cathode-current densities are accordingly enhanced with the increasing H_2O_2 concentration from 0 to 3 mM, which revealed that MoS_2/CC is suitable for construction of the electrochemical biosensors due to its efficient electrocatalytic performance. According to the former research,[34] we hypothesize that the proposed biosensor is based on the following detection mechanism, but the exact mechanism is not completely understood and needs further investigation. MoS_2/CC as a good electron conductor facilitates the electron transfer from the MoS_2/CC electrode to reduce H_2O_2.

$$MoS_{2\,(Ox)} + e^- \leftrightarrows MoS_{2\,(Red)} \quad (1)$$

$$MoS_{2\,(Red)} + 2H_2O_2 \leftrightarrows MoS_{2\,(Ox)} + 2H_2O + O_2 \quad (2)$$

The CV curves of MoS_2/CC were plotted within the range of 10–200 mV s^{-1} in 0.1 M PBS containing 1 mM H_2O_2 (Fig. 2c). As shown in Fig. 2c, the current densities at the cathode and the anode augment continuously upon increasing the scan rates by CV scanning. Obviously, both anodic and cathodic current densities are proportional to the scan rates (Fig. 2d), indicating that the process of electrochemical reduction follows a typical absorption control mechanism.[35,36]

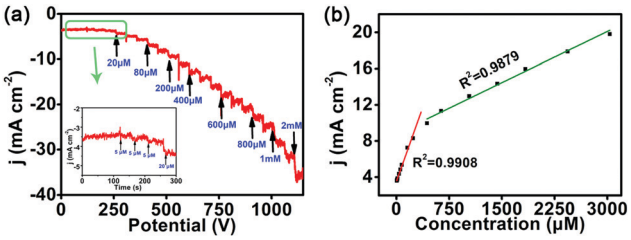

Fig. 3 (a) Amperometric response of MoS_2/CC to the successive addition of H_2O_2 in 0.1 M PBS (pH = 7.4). Applied potential: −0.5 V. The inset shows the amperometric response of H_2O_2 at low concentration. (b) Calibration curve of current response *vs.* H_2O_2 concentration.

Before electrochemical sensing, it is important to achieve the most appropriate reduction potential by chronoamperometry. The optimum applied potential for the electrochemical sensing requires two factors: (i) a larger current response and (ii) a lower signal-to-noise ratio. Fig. S4 (ESI†) shows the amperometric current response of the biosensor with the successive addition of 1 mM H_2O_2 into the stirring PBS at different potentials. According to current–time (*i*–*t*) curves, −0.5 V was chosen as the best potential for subsequent experiments. After this, the current response of MoS_2/CC for H_2O_2 sensing with the successive addition of H_2O_2 into the electrolyte solution was monitored at −0.5 V to assess the sensitivity for electrochemical detection. As shown in Fig. 3a, the fast current response can be observed with the increase in the H_2O_2 concentration and the current platforms were steady within 3 s. The inset of Fig. 3a shows the amplified amperometric response of H_2O_2 in the low concentration region. Accordingly, Fig. 3b presents the linear functional relationship of current density *vs.* H_2O_2 concentration in the range of 5.0 to 3.0×10^3 μM. There are two linear calibration plots corresponding to the low (5.0–2.35×10^2 μM) and medium (4.35×10^2–3.0×10^3 μM) concentration ranges. They are in good fit with the regression equations of $j = 3.53 + 0.0218 \times C_{H_2O_2}$ ($R^2 = 0.9908$) and $j = 8.81 + 0.0038 \times C_{H_2O_2}$ ($R^2 = 0.9879$), respectively. In particular, the sensitivity in the two concentration ranges is as high as 5.3 and 3.6 mA mM^{-1} cm^{-2}, respectively. Furthermore, the detection limit is estimated to be 1.0 μM (S/N = 3), suggesting that the proposed biosensor is superior than a number of recently developed electrochemical H_2O_2 sensors (Table S1, ESI†).

Lung cancer is one of the most common malignancies worldwide and poses a serious security threat to people's life and health.[37] Hence, we chose A549 cells as model cells to check the possibility of practical application of MoS_2/CC to detect H_2O_2 in this work. Phorbol-12-myristate-13-acetate (PMA) was used to stimulate the production of H_2O_2 in cells.[38,39] As depicted in Fig. 4, the amperometric current density response increased apparently upon adding PMA into 20 mL of PBS (pH = 7.4) containing 4×10^7 cells, while no signal could be observed if the cells were not treated with PMA. This phenomenon proves that the recorded current originates from the reduction of H_2O_2, released from A549 cells upon being stimulated. In summary, the developed MoS_2/CC biosensor is suitable for real-time monitoring of extracellular H_2O_2 for clinical research.

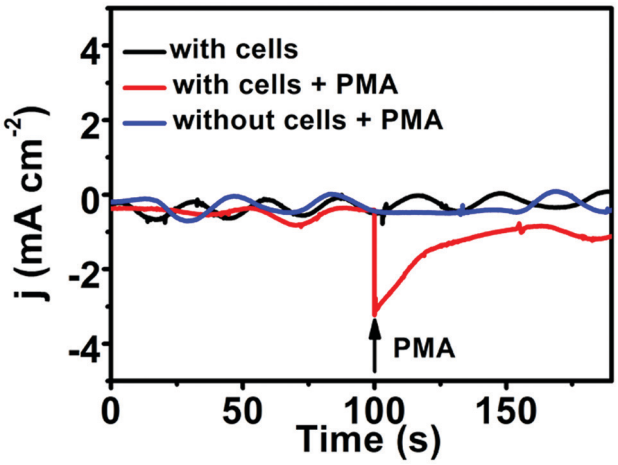

Fig. 4 Amperometric response of MoS_2/CC to the stimulation in 0.1 M PBS (pH = 7.4) with and without A549 cells. Applied potential: −0.5 V.

Considering the practical application, the selectivity and stability are equally crucial as major factors of the analytical properties. The current change upon injection of some interfering substances (such as AA, UA, DA, NaCl, and L-Cys) and H_2O_2 into PBS successively at −0.5 V is compared to assess the specificity of the proposed biosensor. As presented in Fig. S5 (ESI†), the current responds obviously towards H_2O_2, while the response is negligible to the variation in the concentration of other interferences. The anti-interference test suggests that the MoS_2/CC electrode exhibits acceptable selectivity for H_2O_2. The stability of the MoS_2/CC biosensor is evaluated by recording successive CV responses of 1.0 mM H_2O_2 20 times. As shown in Fig. S6 (ESI†), the current density only presents slight loss during multiple cycles in 0.1 M PBS containing 1.0 mM H_2O_2, suggesting the satisfying stability of the proposed biosensor.

In conclusion, MoS_2 nanoarrays directly grown on carbon cloth were prepared and their electrochemical sensing ability towards H_2O_2 was explored. The obtained MoS_2/CC biosensor exhibits attractive electrocatalytic activity with a low detection limit and excellent sensitivity and selectivity due to its abundant surface area and low charge transfer resistance. More significantly, a non-enzymatic H_2O_2 biosensor based on the as-prepared MoS_2/CC exhibits extremely high sensitivity in determination of the trace H_2O_2 amount secreted from A549 cells. This study opens up an avenue for the application of self-supported nanoarrays in the field of electrochemical sensing.

This work was supported by the National Natural Science Foundation of China (21775089 and 21671118), the Outstanding Youth Foundation of Shandong Province (ZR2017JL010), the Key Research and Development Program of Jining City (2018ZDGH032) and Taishan scholar of Shandong Province.

Conflicts of interest

There are no conflicts to declare.

References

1 X. Xiong, C. You, X. Cao, L. Pang, R. Kong and X. Sun, *Electrochim. Acta*, 2017, **253**, 517–521.
2 T. Marimuthu, M. R. Mahmoudian, S. Mohamad and Y. Alias, *Sens. Actuators, B*, 2014, **202**, 1037–1043.
3 B. Dou, J. Yang, R. Yuan and Y. Xiang, *Anal. Chem.*, 2018, **90**, 5945–5950.
4 Y. Zhang, J. Xiao, Q. Lv, L. Wang, X. Dong, M. Asif, J. Ren, W. He, Y. Sun, F. Xiao and S. Wang, *ACS Appl. Mater. Interfaces*, 2017, **9**, 38201–38210.
5 P. Mroz, J. Bhaumik, D. K. Dogutan, Z. Aly, Z. Kamal, L. Khalid, H. L. Kee, D. F. Bocian, D. Holten, J. S. Lindsey and M. R. Hamblin, *Cancer Lett.*, 2009, **282**, 63–76.
6 S. G. Rhee, *Science*, 2006, **312**, 1882–1883.
7 R. Zhang and W. Chen, *Biosens. Bioelectron.*, 2017, **89**, 249–268.
8 T. Zhang, Y. Gu, C. Li, X. Yan, N. Lu, H. Liu, Z. Zhang and H. Zhang, *ACS Appl. Mater. Interfaces*, 2017, **9**, 37991–37999.
9 J. Chen, X. Ji and Z. He, *Anal. Chem.*, 2017, **89**, 3988–3995.
10 M. Ren, B. Deng, J. Wang, X. Kong, Z. Liu, K. Zhou, L. He and W. Lin, *Biosens. Bioelectron.*, 2016, **79**, 237–243.
11 C. J. MacNevin, T. Watanabe, M. Weitzman, A. Gulyani, S. Fuehrer, N. K. Pinkin, X. Tian, F. Liu, J. Jin and K. M. Hahn, *J. Am. Chem. Soc.*, 2019, **141**, 7275–7282.
12 M. Wang, Z. Mao, T. S. Kang, C. Y. Wong, J. L. Mergny, C. H. Leung and D. L. Ma, *Chem. Sci.*, 2016, **7**, 2516–2523.
13 Z. Mao, M. Wang, J. Liu, L. J. Liu, S. M. Y. Lee, C. H. Leung and D. L. Ma, *Chem. Commun.*, 2016, **141**, 4450–4453.
14 X. Wang, P. Li, Q. Ding, C. Wu, W. Zhang and B. Tang, *J. Am. Chem. Soc.*, 2019, **141**, 2061–2068.
15 S. Chaiyo, E. Mehmeti, W. Siangproh, T. L. Hoang, H. P. Nguyen, O. Chailapakul and K. Kalcher, *Biosens. Bioelectron.*, 2018, **102**, 113–120.
16 L. Monti, S. Negri, A. Meucci, A. Stroppa, A. Galli and G. Contarini, *Food Chem.*, 2017, **220**, 18–24.
17 Y. Huang and W. Liu, *J. Pharm. Biomed. Anal.*, 2005, **38**, 537–542.
18 A. M. Almuaibed and A. Townshend, *Anal. Chim. Acta*, 1994, **295**, 159–163.
19 C. Dong, H. Zhong, T. Kou, J. Frenzel, G. Eggeler and Z. Zhang, *ACS Appl. Mater. Interfaces*, 2015, **7**, 20215–20223.
20 S. Wang, L. Zhang, S. Wan, S. Cansiz, C. Cui, Y. Liu, R. Cai, C. Hong, L. Teng, M. Shi and Y. Wu, *ACS Nano*, 2017, **11**, 3943–3949.
21 F. Wei, P. Patel, W. Liao, K. Chaudhry, L. Zhang, M. Arellano-Garcia, S. Hu, S. Shukla and F. Shah, *Clin. Cancer Res.*, 2009, **15**, 4446–4452.
22 M. G. Walter, E. L. Warren, J. R. McKone, S. W. Boettcher, Q. Mi, E. A. Santori and N. S. Lewis, *Chem. Rev.*, 2010, **110**, 6446–6473.
23 H. Du, R. Kong, F. Qu and L. Lu, *Chem. Commun.*, 2018, **54**, 10100–10103.
24 H. Du, X. Guo, R. Kong and F. Qu, *Chem. Commun.*, 2018, **54**, 12848–12851.
25 H. Liu, S. Han, Y. Zhao, Y. Zhu, X. Tian, J. Zeng, J. Jiang, B. Xia and Y. Chen, *J. Mater. Chem. A*, 2018, **6**, 3211–3217.
26 B. Hinnemann, P. G. Moses, J. Bonde, K. P. Jørgensen, J. H. Nielsen, S. Horch, I. Chorkendorff and J. K. Nørskov, *J. Am. Chem. Soc.*, 2015, **127**, 5308–5309.
27 D. Voiry, M. Salehi, R. Silva, T. Fujita, M. Chen, T. Asefa, V. Shenoy, G. Eda and M. Chhowalla, *Nano Lett.*, 2013, **13**, 6222–6227.
28 T. Wang, H. Zhu, J. Zhuo, Z. Zhu, P. Papakonstantinou, G. Lubarsky, G. Lin and M. Li, *Anal. Chem.*, 2013, **85**, 10289–10295.
29 Y. Shu, W. Zhang, H. Cai, Y. Yang, X. Yu and Q. Gao, *Nanoscale*, 2019, **11**, 6644–6653.
30 Y. Gou, Q. Liu, X. Shi, A. M. Asiri, J. Hu and X. Sun, *Chem. Commun.*, 2018, **54**, 5066–5069.
31 R. Zhang, J. Ma, W. Wang, B. Wang and R. Li, *J. Electroanal. Chem.*, 2010, **643**, 31–38.
32 W. Zhu, C. Tang, D. Liu, J. Wang, A. M. Asiri and X. Sun, *J. Mater. Chem. A*, 2016, **4**, 7169–7173.
33 Z. Pu, Q. Liu, A. M. Asiri, Y. Luo, X. Sun and Y. He, *Electrochim. Acta*, 2015, **168**, 133–138.
34 B. Sherino, S. Mohamad, S. N. A. Halim and N. S. A. Manan, *Sens. Actuators, B*, 2018, **254**, 1148–1156.
35 F. Xie, X. Cao, F. Qu, A. M. Asiri and X. Sun, *Sens. Actuators, B*, 2018, **255**, 1254–1261.
36 X. Zhang, W. Guo, Z. Wang, H. Ke, W. Zhao, A. Zhang, C. Huang and N. Jia, *Sens. Actuators, B*, 2017, **253**, 470–473.
37 N. Li, L. Jia, R. Ma, W. Jia, Y. Lu, S. Shi and H. Wang, *Biosens. Bioelectron.*, 2017, **89**, 453–460.
38 A. W. Griffith and J. M. Cooper, *Anal. Chem.*, 1998, **70**, 2607–2612.
39 X. Li, Y. Liu, A. Zhu, Y. Luo, Z. Deng and Y. Tian, *Anal. Chem.*, 2010, **82**, 6512–6518.